Effect of the Solvent Polarity and Temperature in the Isolation of Pure Andrographolide from *Andrographis paniculata*

Rahul Maurya[1*], Thirupataiah B[1], Lakshminarayana Misro[1], Thulasi R[1], Rajeesh VR[1] and Rohit KS[1]

National Ayurveda Research Institute for Panchakarma, Cheruthuruthy, Thrissur, Kerala, 679 531
*Corresponding author: mauryabrahul@gmail.com

ABSTRACT

The primary objective of the proposed research work is to extract and enrich pure andrographolide (AGL) by varying the polarity index and Hildebrand solubility parameter (δ) of a moderately polar solvent. Both parameters affect the solubility of AGL in different solvents and extraction methods.

AGL was extracted from the whole plant *Andrographis paniculata*. Continuous or Direct, Maceration and Soxhlet extraction method used for extraction. Based on the appearance of the crystal in the direct Soxhlet ethyl acetate method, their yield was further optimized by using a randomized response surface methodology (RSM) and quadratic model-based Box–Behnken design (BBD). HPTLC was used to determine the AGL extraction efficiency, purity, and quantification. Based on the obtained result, the pure andrographolide crystal (yield 0.185 g/g) was obtained by direct Soxhlet extraction. Ethyl acetate is used as a solvent. The R_f exhibited in the TLC chromatogram was 0.28. The FT-IR spectra exhibited characteristic peaks similar to the standard AGL, and ^{1}H-NMR and ^{13}C NMR elucidated the crystal structure. The DEPT -90/135 spectra showed that the extracted crystal was pure AGL. One of the novel approaches is isolating pure AGL crystals in a moderately polar solvent (ethyl acetate) by elevating the Hildebrand solubility parameter despite using polar solvents. AGL crystals were obtained from direct Soxhlet extraction by ethyl acetate.

It is a single-step and more economical method. It can be easily transformed into a pilot or industrial setup to extract the pure AGL.

Keywords: *Andrographis paniculata,* Andrographolide, Soxhlet, NMR, HPTLC, Crystal.

INTRODUCTION

Andrographolide (AGL) is an active phytoconstituent of *Andrographis paniculata*. Chemically, it is a diterpenoid lactone ring (Rahul, Boini, Lakshminarayana, Radhakrishnan, & Sudayadas, 2022). Due to the variable solubility and polarity of AGL in different solvents, it cannot be purely isolated by reported methods (Rubi et al., 2019). Microwave, ultrasonic, and supercritical fluid-assisted extraction techniques were used for AGL high-yield extraction. However, further chromatographic separation (Column, Flash Chromatography) was needed to obtain pure AGL. Although these are modern, sophisticated

techniques, they require multiple stages to obtain a pure compound. In the present scenario, the essential key factor in the field of herbal technology is the extraction of a single compound in a single-step process, rather than the high-yield extraction of multiple components followed by the numerous separation techniques used to obtain pure compounds. Extraction techniques can quickly isolate a single phytoconstituent by simulating the solvent's polarity index value or Hildebrand solubility parameter (δ) to the respective bioactive compounds (Ballesteros-Vivas et al., 2019). Solubility plays a vital role in the extraction of the compound. Hildebrand's

solubility parameter (δ) states that the solubility of any bioactive compound in any solvent is based on its polarity or solubility parameter (Sohani et al., 2021). The square root of the cohesive energy density is expressed as the Hildebrand solubility parameter (δ), which describes the ratio of the heat of vaporization to the molar volume of the compound at a definite temperature (Sodeifian, Alwi, Razmimanesh, & Tamura, 2021). This research comprises different approaches to enhance AGL extraction. To improve the extraction of pure AGL, various solvents (hexane, Pet. Ether, toluene, ethyl acetate, and methanol) and methods (direct/continuous; cold maceration/Soxhlet) were used; among these, the best solvent (ethyl acetate) and method (direct Soxhlet) were selected based on the obtained AGL crystal. The parameter of the selected method was optimized to increase the yield of pure AGL. Variations in temperature and the nature of the solvent influence the extraction of AGL(Liu et al., 2022). In the modern era, along with extraction, the isolation of a single bioactive compound is a significant concern. Various novel extraction techniques have been developed, such as microwave and supercritical fluid extraction. However, this method is not cost-effective regarding technology transfer to industrial setups concerning conventional methods. The research is based on developing a single-state cost-effective extraction method for a single bioactive compound enhancing the Hildebrand solubility parameter of a moderately polar solvent. At elevated temperatures, it plays a significant role in the solubility of AGL. At a higher heat of vaporization, equilibrium is established between the δ value of the solvent and solute; as a result, the solubility of the solute increases (Mood Mohan et al., 2022). However, at ambient temperature, the δ values of the solute and solvents differ, which subsequently affects the crystal formation of the solute.

MATERIALS AND METHODS

Materials

Plant Material: *Andrographis paniculata* was collected from the local geographical area Pattambi, Kerala, and authenticated (ACCESSION No. 205). The whole plant was dried at ambient temperature for a day and then kept in a hot-air oven below 60 °C. It was ground to a 40 mesh powder and appropriately stored for further use: hexane, Pet. Ether, toluene, ethyl acetate, and methanol were purchased from Merck, India. Andrographolide standards were purchased from Nature remedies, Bangalore, India (purity > 95% by HPLC), and precoated silica gel plate 60 F_{254} was purchased from Merck, India.

Extraction and Isolation

Extraction was performed with slight modification in the method reported by Rajani *et al*. The whole dried plant of *A. paniculata* converted into the coarse powder was subjected to extraction by two different methods (Table 01) (Direct and Continuous; Cold Maceration and Soxhlet extraction) (Paul, Vibhuti, & Raj, 2021). In continuous cold maceration and Soxhlet, different solvents (hexane, petroleum ether, toluene, ethyl acetate, and methanol) were used in increasing polarity order (Barwick, 1997). However, in direct cold maceration and Soxhlet extraction, ethyl acetate and methanol were used as solvents. Based on crystal yield, direct Soxhlet extraction in ethyl acetate was selected, and the extraction parameter (solute: solvent) proportion, temperature, and extraction time were optimized using design expert software version 13. Randomized response surface (RSM) and quadratic model-based Box–Behnken design (BBD) were used for the optimization of independent variables: proportion of solvent for 1 part of solute (50 g), temperature (°C), and time (Minute) at three coded levels (-1) low, (0) moderate and (+1) high to obtain a maximum response in terms of % yield (w/w) and % andrographolide (w/w) (Table 02 and Supplementary data Table 01). Seventeen experimental runs with five central points were performed (Supplementary information 1). A relation between the independent variable and dependent response is expressed by polynomial Eq (1)

$$Y1/Y2 = \beta 0 + \beta 1\,A + \beta 2\,B + \beta 3\,C + \beta 12\,AB + \beta 13\,AC + \beta 23\,BC + \beta 11\,A^2 + \beta 22\,B^2 + \beta 33\,C^2 \quad \dots (01)$$

where Y1 (% yield of extract) and Y2 (% AGL), β0 represent constant β1, β2 and β3 are linear coefficients, β12, β13, and β23 are interaction coefficients, and β11, β22, and β33 are quadratic coefficients. A, B and C are coded values for solvent part, extraction temperature (°C), and extraction time (min.), respectively.

Table 1 Different techniques and modes for the full extraction of Androgrpholide

AGL extraction Technique/Mode	Direct Extraction	Continuous or Successive extraction
Soxhhlet Extraction	Ethyl acetate and Methanol	Hexane, Pet. Ether, Toluene, Ethyl acetate and Methanol
Cold maceration	Methanol, ethyl acetate	Hexane, Pet. Ether, Toluene, Ethyl acetate and Methanol

Table 2 Independent variables and their corresponding levels

Independent variable	Symbol	Coded level		
		-1	0	+1
Solvent for 1 part of solute	A	1	5	10
Temperature (ºC)	B	50	100	150
Time (min.)	C	30	60	90

Identification of andrographolide by HPTLC

Standard andrographolide (0.7 mg) and different extracts were accurately weighed and dissolved in 1 mL of methanol. Precoated silica gel plate 60 F_{254}, (10×10 cm) was used as the stationary phase, and toluene:ethyl acetate:formic acid (5:4.5:0.5 v/v) was used as the mobile phase. The applicator spotted a fixed concentration strength (42 μg) or 60 μL spot of standard along with different extracts and crystals (Camag, Linomat V, Anchrome, Switzerland). Abbreviations of different extracts: Continuous Soxhlet extraction hexane (SH), Continuous Soxhlet extraction Pet ether (SPE), Continuous Soxhlet extraction toluene (ST), Continuous Soxhlet extraction Ethyl acetate (SEA), Continuous Soxhlet extraction Methanol (SM), Continuous Cold Maceration Hexane (CHE), Continuous Cold Maceration Pet. Ether (CPE), Continuous Cold Maceration toluene (CT), Continuous Cold Maceration Ethyl acetate (CEA), and Continuous Cold Maceration Methanol (CM). The direct extract obtained from methanol and ethyl acetate by cold maceration is denoted as S1 and S2, and the direct extract obtained from methanol and ethyl acetate by Soxhlet extraction is denoted as S3 and S4. Crystal obtained from Soxhlet Ethyl acetate extract denoted as S5. The TLC plate was developed by placing the plate in a saturated glass chamber (10×10 cm, Cammag, Anchrome, Switzerland). The glass chamber was saturated with the mobile phase. The plate was dried room temperature and the Camag TLC visualizer captured the HPTLC fingerprint profiler under UV at 254 nm and 366 nm.

Quantification of AGL by HPTLC

The developed TLC plate was scanned (Camag TLC Scanner IV, India) at a wavelength of 254 nm. Detection and data evaluation studies can be performed by Wincats, an integrated Software 4.2. The AUC at the respective R_f was determined for the quantitative investigation of the pure compound in the extract.

Determination of % Purity

The % purity of each tested extraction technique was checked. The obtained dry matter content was expressed in % and calculated from the equation below in Eq. 01

$$\%Purity = \frac{\text{AUC of Extract}}{\text{AUC of Standard andrographolide}}$$

…(Eq. 01)

Identification of andrographolide by FT-IR

An FT-IR spectrophotometer (Agilent, CARY630, Malaysia) was used to identify the functional groups. A small quantity of standard AGL and different dried extracts and crystals was placed into the sample holder, the spectra were run in the range of 4000-600 cm^{-1}, and the intensity of % transmittance was determined. The characteristic frequencies of the standard and test samples were compared to identify compounds.

Structural elucidation of the andrographolide crystal by NMR

^{1}H-NMR, ^{13}C NMR, and distortionless enhancement by polarization transfer (DEPT-90/135) NMR spectrum of the AGL crystal sample (S5) recorded on a Bruker AVANCE Ascend 400 (400 MHz FT-NMR) Spectroscopy in Chemical Science Department of IISER-Berhampur, India, and CD_3OD used as a solvent. Structural elucidation was carried out by interpreting the obtained spectrum.

RESULTS

Extraction of AGL

Based on the selected experimental design, different independent variables, such as the proportion of solvent (ethyl acetate) to 1 part of solute (50 g) coarse powder, were optimized at three levels, as shown in Table 02. The effect of each coefficient on the response is expressed in terms of the positive and negative correlation coefficients given in Eq. 02 and 03. The positive value of the interaction coefficient indicates that extraction and AGL yield increased with increasing their value; a negative value indicates that the response value decreased with increasing variable values. The effect of each interaction coefficient on the response can be expressed by the response surface plot given in **fig. 1.** The optimized value for all the factors was predicted at 8.628 parts ethyl acetate, 124.756 °C temperature, and 66 min. The observed response % extract yield and % of pure AGL crystal w/w were obtained at 19.049% and 0.215 g/g, respectively. It was nearly equal to the predicted value (extraction yield 19.054% and % andrographolide 0.225%). It seems that the proposed model is significant for characteristic responses.

Y_1=18.54 + 2.60A + 1.43B + 0.7421C + 0.1090AB − 0.2097AC + 0.2050BC − 2.96A^2 − 1.50B^2 − 0.6553C^2

…Eq(02)

Y_2 = 0.1884 + 0.0471A + 0.0481B + 0.0439C + 0.0434AB + 0.0407AC + 0.0407BC − 0.0732A2 − 0.0667B2 − 0.0634C^2
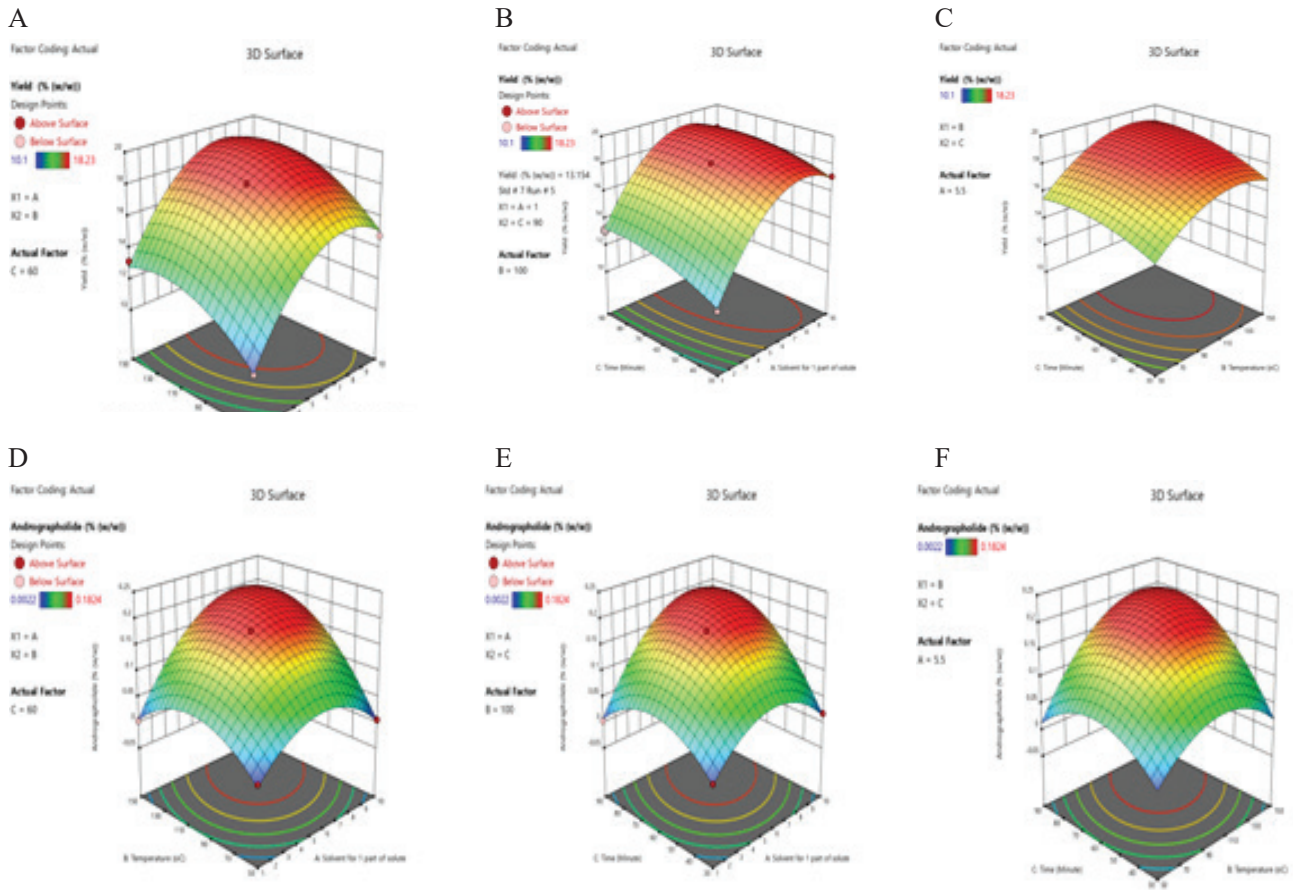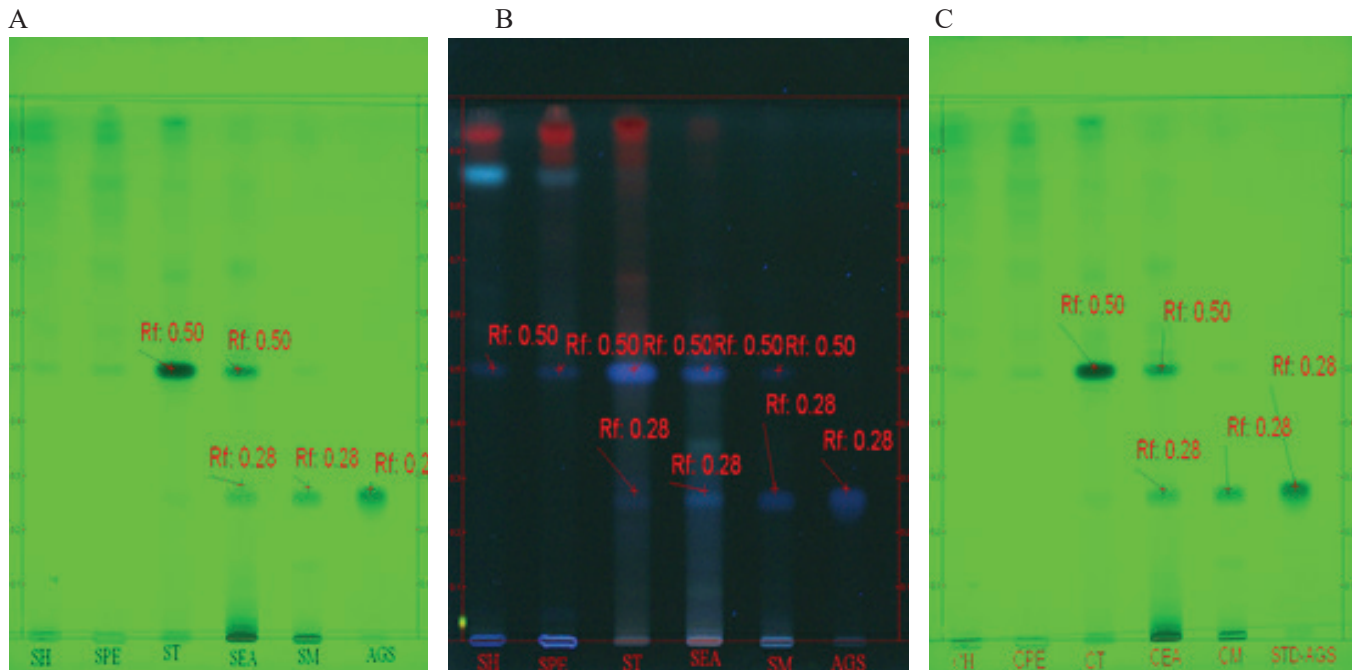
…Eq(03)

Fig. 1 A: Effect of Temperature and Part of Solvent on % (w/w) Yield B: Effect of Time and Part of solvent on % (w/w) Yield C: Effect of Time and Temperature on % (w/w) Yield, D: Effect of Temperature and Part of Solvent on % (w/w) Andrographolide E: Effect of Time and Part of solvent on % (w/w) Andrographolide F: Effect of Time and Temperature on % (w/w) Andrographolide
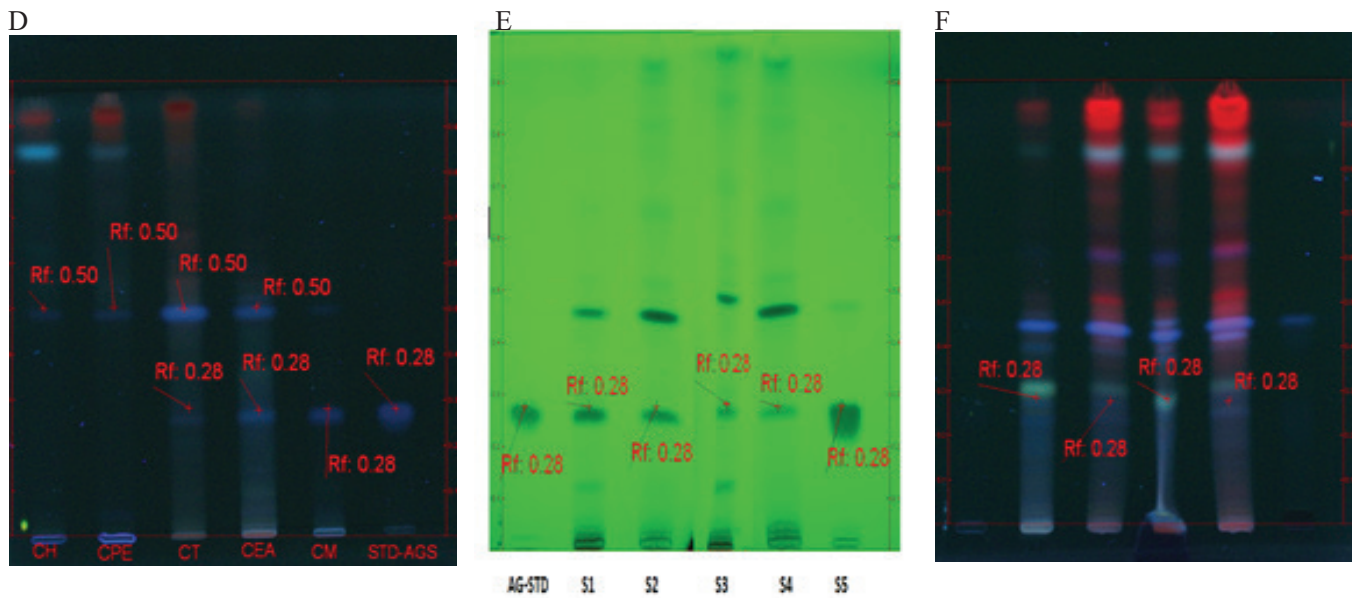
Fig. 2 Identification of AGL by HPTLC Method A: Contunuous Soxhlet extraction at 254 nm, B: Soxhlet-modified hexane to methanol at 366 nm, C: Continuous cold Maceration at 254 nm, D: Continuous cold Maceration at 366 nm, E: Direct Soxhlet extraction and cold maceration at 254 nm, F: Direct Soxhlet extraction and cold maceration at 366 nm
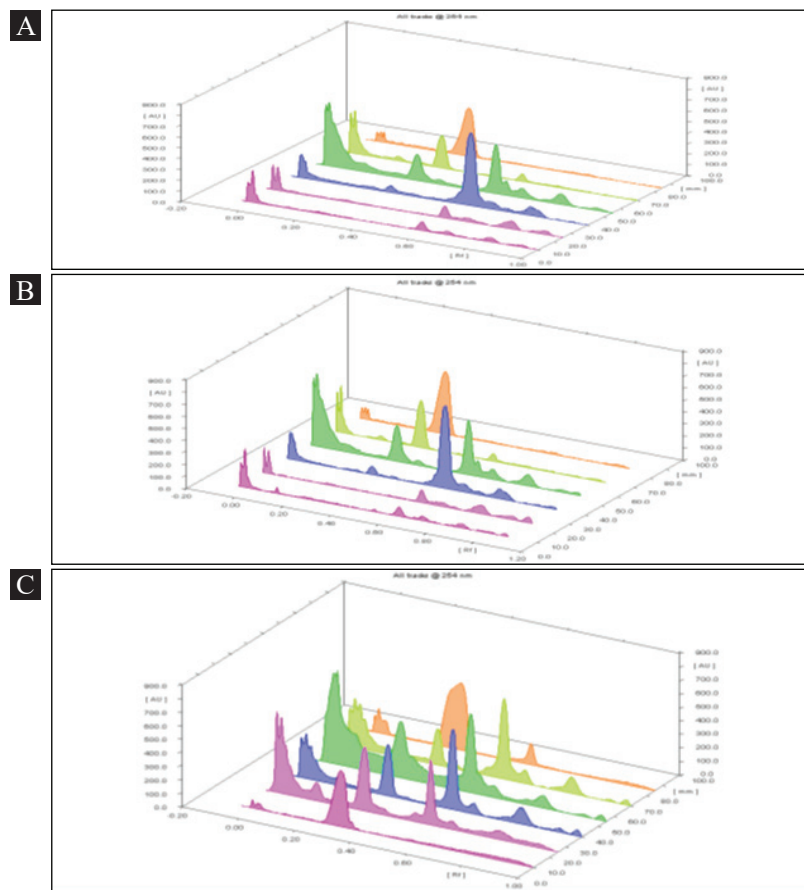

Fig. 3 AUC HPTLC Chromatogram of different Extracts of AGL; A: Continuous Soxhlet extraction, B: Continuous Cold Maceration extraction, C: Direct Soxhlet and cold maceration

Fig. 2 shows that the standard spot appeared at an R_f of 0.28. Spots at similar R_f values appeared in different extracts at 254 and 366 nm. Methanol and ethyl acetate extracts derived from various methods exhibited spots at R_f 0.28 at 254 and 366 nm.

Quantification of AGL by HPTLC
Fig. 3 Exhibited HPTLC chromatogram of standard crystal (S5) and extracted compound obtained from different extraction methods, which appeared at the R_f value of 0.28. The chromatogram showed that Sample S5 (AGL crystal) has a maximum AUC at an R_f of 0.28.

Determination of % Purity
A single spot at R_f 0.28 exhibited that the purest AGL

crystal was obtained from direct Soxhlet extraction in ethyl acetate. Extracts of other methods showed multiple spots in the TLC plate, revealing that it contained multiple compounds along with AGL, so further separation was required to obtain pure compounds (Fig. 4).

Identification of andrographolide by FT-IR
The FT-IR spectra exhibited that characteristic peaks of crystal Sample S5 appear at 3387 cm⁻¹ (-OH stretching), 2925 cm⁻¹ (sp³ C-H stretching), 2846 cm⁻¹ (C-H stretching), 1717 cm⁻¹ (-COOR stretching), and 1669 cm⁻¹ (C=C stretching). Similar peaks were observed in the AGL standard. The FT-IR spectra of other extracts have low-intensity characteristic peaks, as shown in **Fig. 5**.
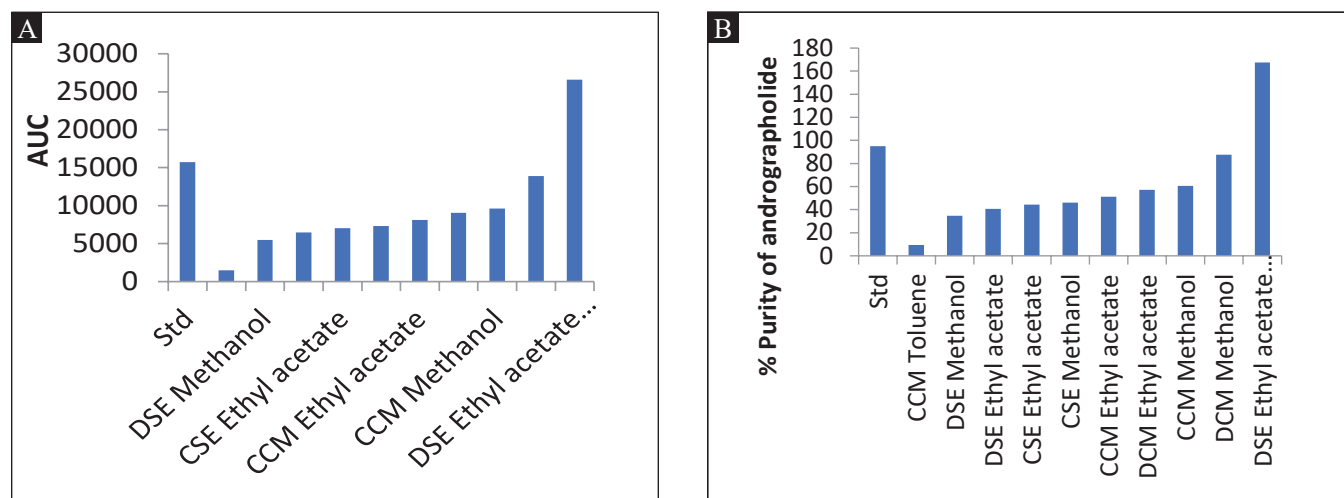

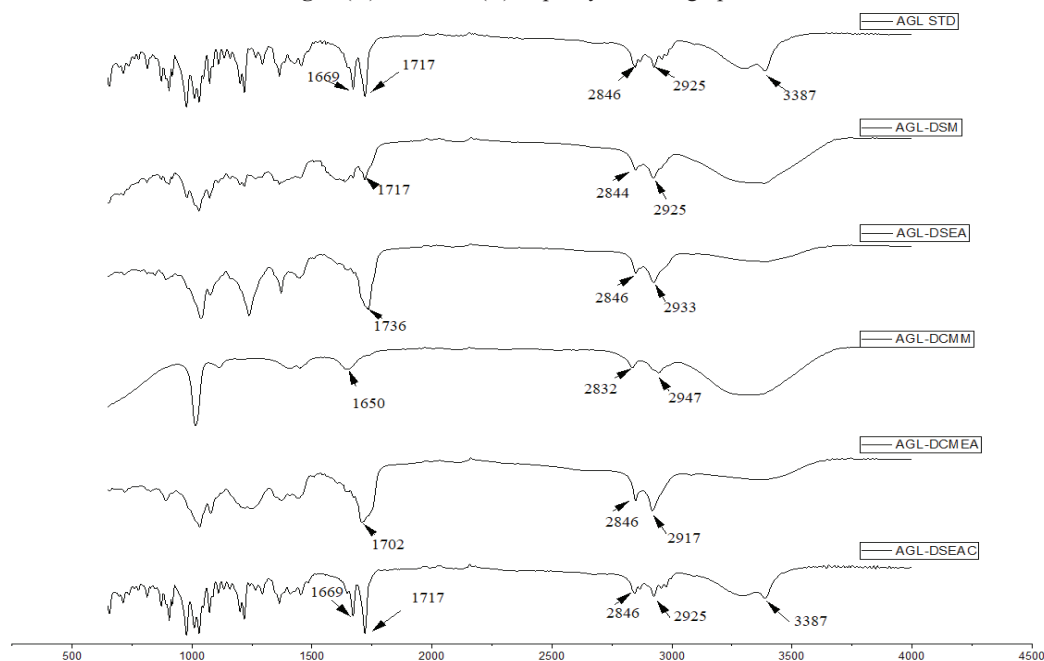**Fig. 4** (A) AUC and (B) % purity of andrographolide

Fig. 5 IR spectra of standard andrographolide and different extract AGL-STD andrographolide standards

AGL-STD Andrographolide standard

AGL-DSM- andrographolide in direct Soxhlet methanol

AGL-DSEA-andrographolide in direct Soxhlet Ethyl acetate

AGL-DCMM-andrographolide in direct cold maceration methanol

AGL-DCEA-andrographolide in direct cold maceration ethyl acetate

AGL-DSEAC-andrographolide in direct Soxhelet ethyl acetate crystals

Structural elucidation of the andrographolide crystal by NMR

^{1}H-NMR spectra: **Fig. 6A and 6B** exhibit characteristic signals at δ 6.85 (t, 1H), 5.03 (d, J = 5.8 Hz, 1H), 4.91 (s, 1H), 4.69 (s, 1H), 4.48 (dd, J = 10.2, 6.1 Hz, 1H), 4.20 – 4.09 (m, 2H), 3.48 – 3.35 (m, 2H), 2.71 – 2.52 (m, 2H), 2.49 – 2.38 (m, 1H), 2.04 (td, J = 13.0, 8.1 Hz, 1H), 1.97 – 1.91 (m, 1H), 1.84 (ddd, J = 18.5, 13.0, 3.6 Hz, 4H), 1.45 – 1.27 (m, 3H), 1.25 (d, J = 8.4 Hz, 3H), 0.77 (s, 3H).
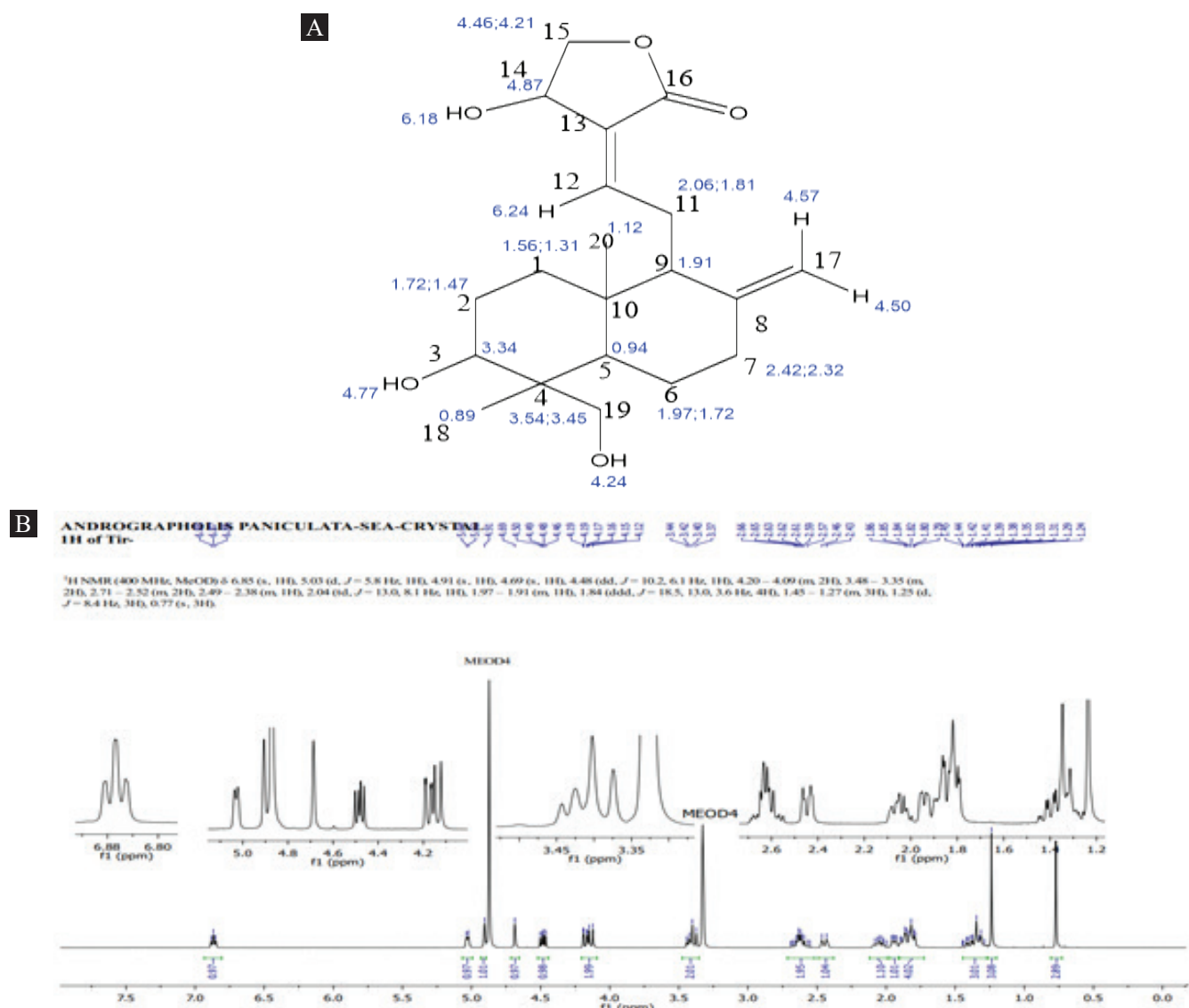

Fig. 6 (A) Estimated ^{1}H NMR Signals of AGL from Chem Draw Professional, (B) Proton NMR spectra of the AGL crystal obtained from direct Soxhlet Ethyl acetate

^{13}C NMR **Fig. 7A and 7B** spectra exhibited signals at δ 171.24, 147.93, 147.39, 128.41, 107.81, 79.53, 74.73, 65.26, 63.58, 56.01, 54.94, 48.23, 48.02, 47.80, 47.59, 47.38, 47.16, 46.95, 42.29, 38.57, 37.58, 36.74, 27.64, 24.31, 23.81, 21.97, 14.13.
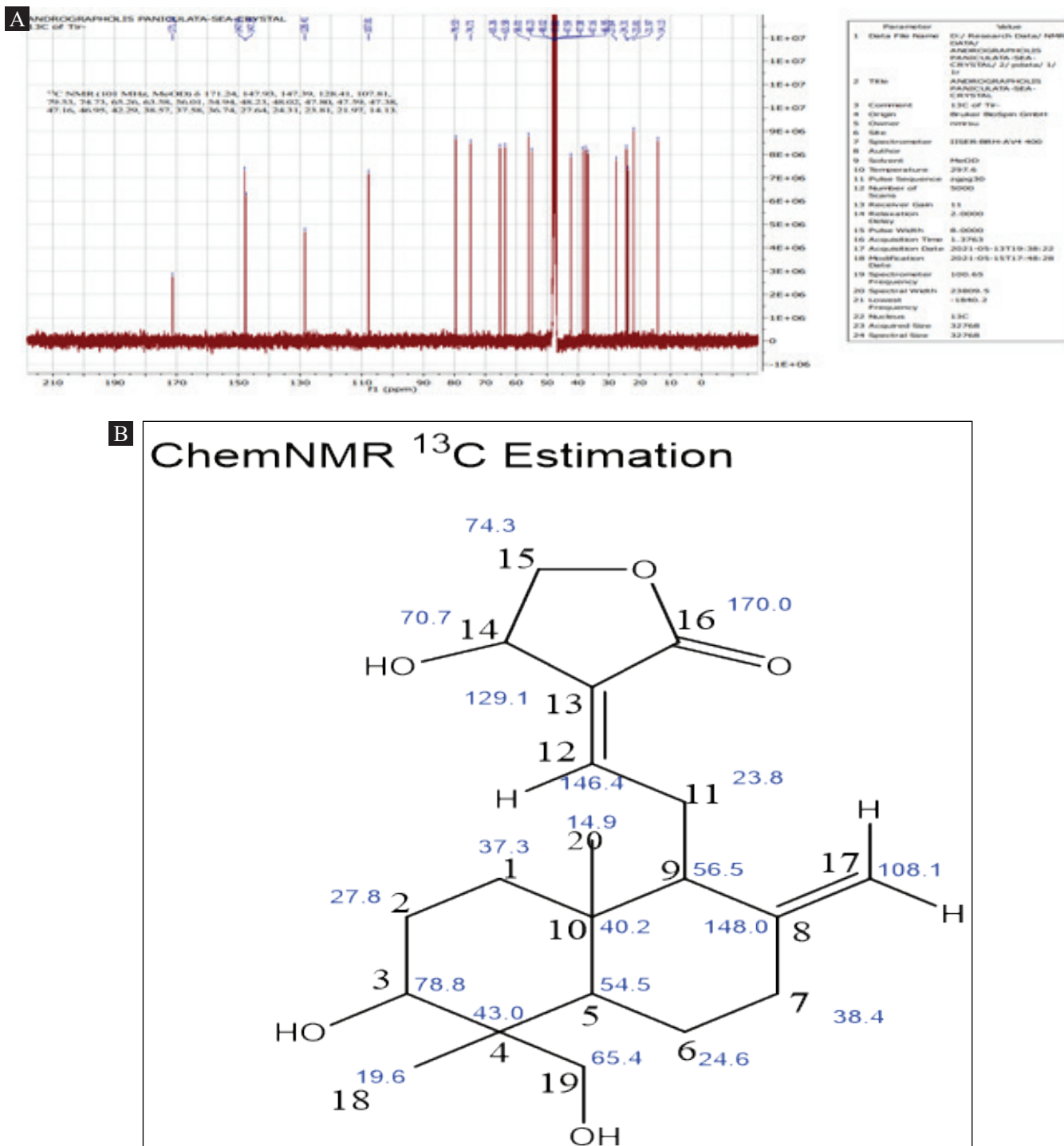
Fig. 7 (A) ^{13}C NMR AGL crystal obtained from direct Soxhlet Ethyl acetate, (B) Estimated ^{13}C NMR Signals of AGL from Chem Draw Professional

DEPT-90/135 NMR: The obtained crystal sample was further analyzed by DEPT-90/135 NMR, as shown in **Fig. 8, and 9** significant differences were observed in DEPT-135 and DEPT-90; the spectrum of DEPT-135 shows positively (-CH3) methyl groups, methine (-CH) carbons and negatively charged methylene (-CH2) carbons, and no further quaternary carbon (C) signals were observed (Mahato & Kundu, 1994). Both DEPT-90 and 135 signals and chemical shift values are given in Table 03, similar to previously reported data of Qi Zhen D et al.(Du Q, 2003) and Chen ZG at all (Z. G. Chen, R. X. Tan, & L. Cao, 2009).

Table 3 Chemical shift variation of the DEPT-90/135 AGL crystal

S.NO.	Carbon Position	Chemical Shift δ (ppm)			
		Andrographolide in CD$_3$OD (^{13}C-Present Study)	Andrographolide in CD$_3$OD (DEPT-135 Present study)	Andrographolide in CD$_3$OD (DEPT-90 Present Study)	Chem Draw Professional prediction for Andrographolide
1	C-1	37.58	37.57 (-VE)	NO SIGNAL	37.3
2	C-2	27.64	27.64 (-VE)	NO SIGNAL	27.8
3	C-3	79.53	79.52 (+VE)	79.52 (+VE)	78.8
4	C-4	42.29	NO SIGNAL	NO SIGNAL	43.0
5	C-5	54.94	54.93 (+VE)	54.93 (+VE)	54.5
6	C-6	24.31	24.31 (-VE)	NO SIGNAL	24.6
7	C-7	36.74	36.73 (-VE)	NO SIGNAL	38.4
8	C-8	147.93	NO SIGNAL	NO SIGNAL	148.0
9	C-9	56.01	56.00 (+VE)	56.00 (+VE)	56.5
10	C-10	38.57	NO SIGNAL	NO SIGNAL	40.2
11	C-11	23.81	23.81 (-VE)	NO SIGNAL	23.8
12	C-12	147.39	147.94 (+VE)	147.94 (+VE)	146.4
13	C-13	128.41	NO SIGNAL	NO SIGNAL	129.1
14	C-14	65.26	65.25 (+VE)	65.25 (+VE)	70.7
15	C-15	74.73	74.74 (-VE)	NO SIGNAL	74.3
16	C-16	171.24	NO SIGNAL	NO SIGNAL	170.0
17	C-17	107.81	107.82 (-VE)	NO SIGNAL	108.1
18	C-18	21.97	21.97 (+VE)	NO SIGNAL	19.6
19	C-19	63.58	63.58 (-VE)	NO SIGNAL	65.4
20	C-20	14.13	14.13 (+VE)	NO SIGNAL	14.9
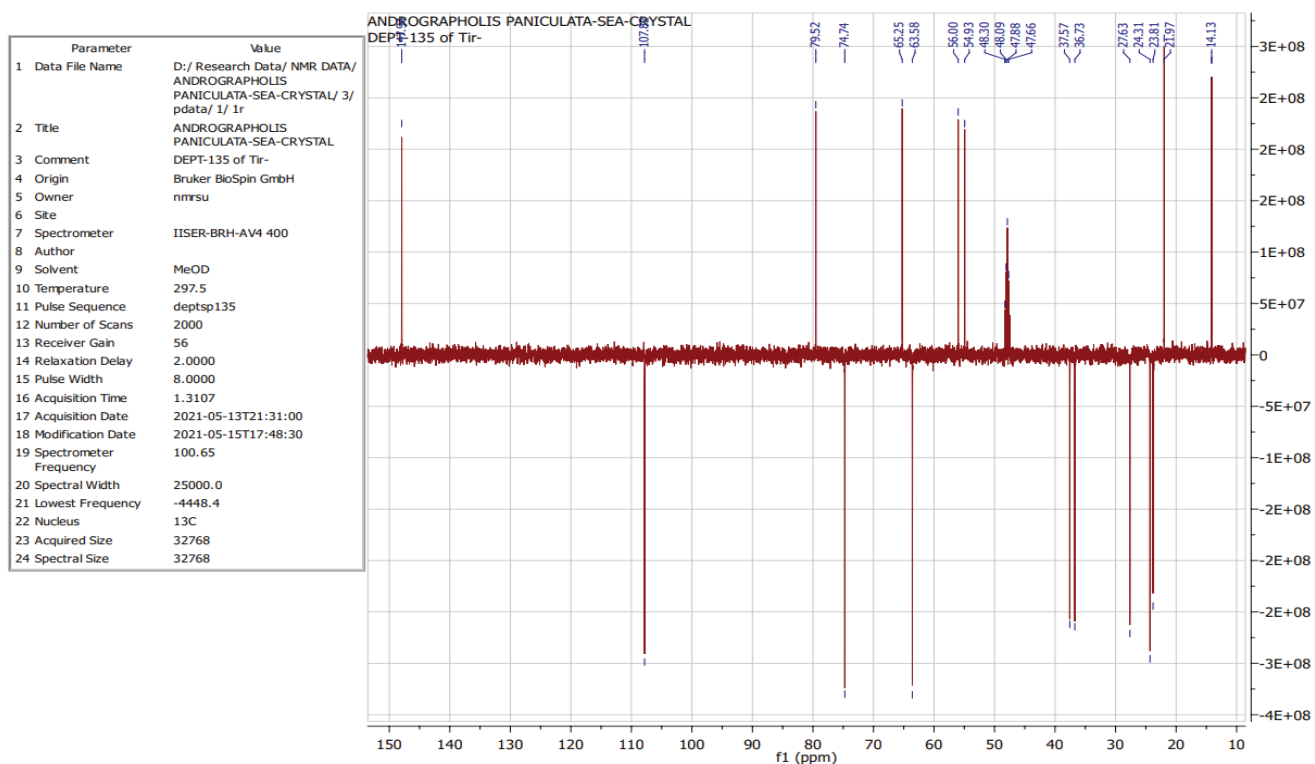
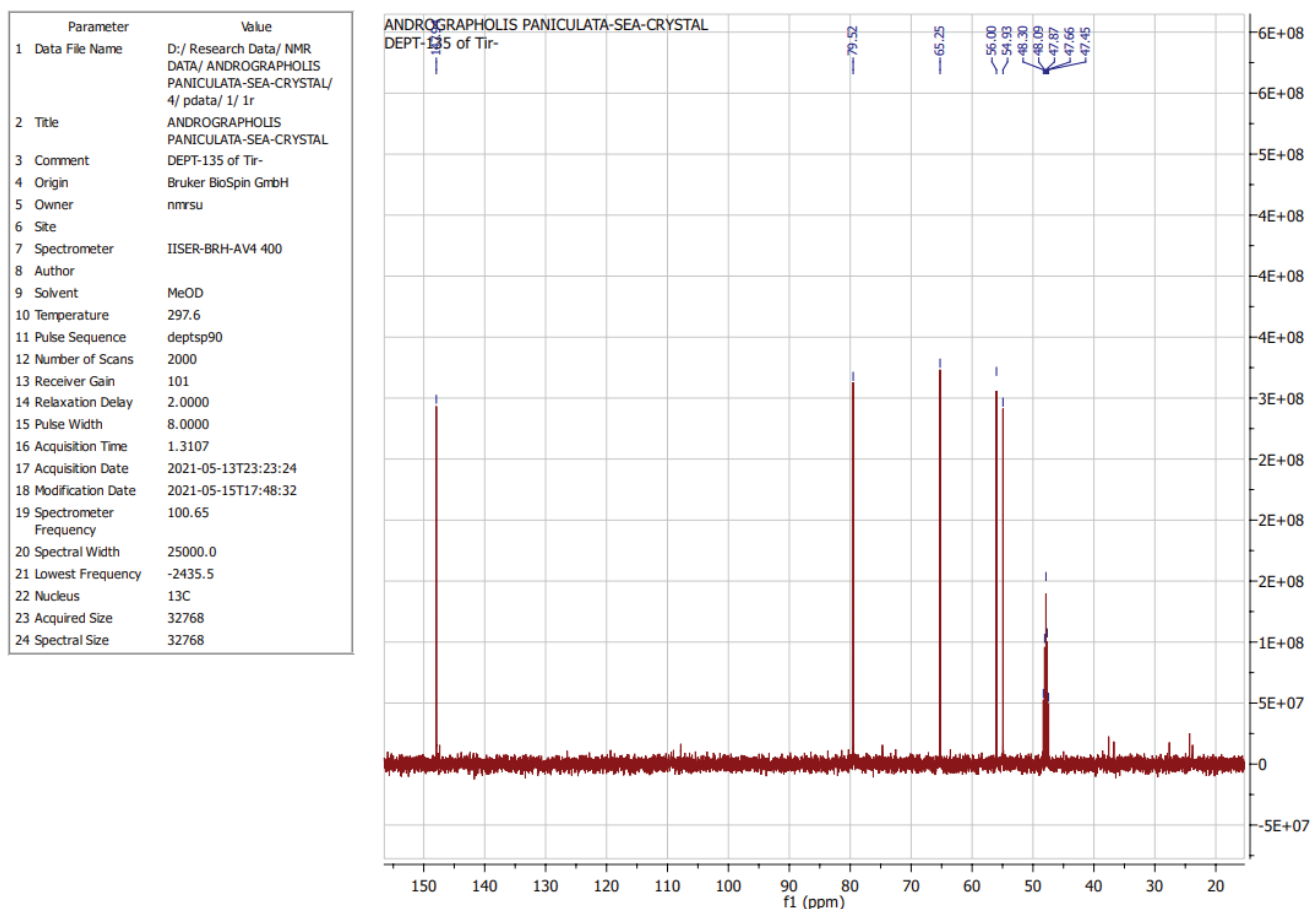**Fig. 8** DEPT-135 Estimated ^{1}H NMR Signals of AGL

Fig. 9 DEPT-90 Estimated ^{1}H NMR Signals of AGL

DISCUSSION

Extraction of AGL

The polarity of the solvent is an essential factor affecting plant material extraction. The extraction efficiency of phytoconstituents increases with increasing solvent polarity (Lapornik et al., 2005; Rafinska et al., 2019) (Lapornik, Prošek, & Wondra, 2005; Rafińska et al., 2019). Pure crystals were obtained in direct Soxhlet extraction by ethyl acetate compared to other solvents and techniques. Kumoro et al. reported that 0.0174 g/g AGL was obtained after the chromatographic separation of 0.58% of the total extract (Kumoro & Hasan, 2007). Mohan et al. also reported 0.16 g/g AGL extraction by microwave followed by the separation technique (Manvitha Mohan, Khanam, Shivananda, & Phytochemistry, 2013). Similarly, Sharma et al. also reported the extraction of AGL in methanol by using ultrasonication and microwave followed by a separation technique to obtain pure AGL (Sharma & Sharma, 2018). However, the optimized method produces more AGL yield (0.215 g/g) in a single-step process with high yield and % purity, along with being cost-effective compared to reported methods so that, it can be easily transformed into the industry for bulk production.

As a Hildebrand solubility parameter (δ), different solvents, such as methanol and ethyl acetate, are used to extract AGL. Cohesive energy can be expressed as the ratio of vaporization energy to molar volume at a fixed temperature and total intermolecular interaction (Roth, 2019). Intermediate polar solvents (ethyl acetate, dichloromethane, and chloroform) could not significantly extract the diterpenoid lactones at ambient temperature. However, the solute dissolved, and its boiling point increased due to its colligative property. At an elevated boiling point, the heat of vaporization of the solvent also increases. This may increase the value of the Hildebrand solubility parameter. At a certain period, the δ values of ethyl acetate and AGL become equal; the solubility of AGL increases in ethyl acetate. However, at ambient temperature, the heat of vaporization and the δ value of ethyl acetate decrease; as a result, a significant difference occurs in the δ value of ethyl acetate and AGL, which would lead to the formation of AGL crystals.

In andrographolide extraction, ethyl acetate, a moderately polar solvent with a high content of -COO groups, was more effective than methanol at elevated temperatures. The value of the polarity index of ethyl acetate increases with temperature and becomes equal to the polarity index of AGL; as a result, the solubility of AGL increases in hot ethyl acetate, and upon cooling, it is precipitated and gives the AGL crystal in a single step.

At ambient temperature, the δ values of methanol and AGL are 14.45 and 14.80, respectively. Solute solubility is maximum when the solute and solvent have the same δ. Therefore, AGL remains present in a solubilized form in methanol at ambient and high temperatures(Rezaei, Rahimpour, Zhao, Martinez, & Jouyban, 2021). Crystals were not observed in methanol compared to ethyl acetate. The isolation of pure AGL in methanol requires further separation by chromatography (column, flash), so single-stage isolation cannot be achieved by methanol or solvents with similar δ values.

The Pure AGL crystal was observed in Direct Soxhlet Ethyl acetate compared to Cold Maceration because the δ value of Ethyl acetate matches the AGL at elevated temperature. The results of the purity percentage are shown in **fig. 4**. The results indicate that extraction of AGL is effective with ethyl acetate Soxhlet extraction rather than other solvents and methods.

Analysis of variance showed that (P< 0.0001) the regression coefficients were 0.9959 and 0.9986 for extraction yield and AGL yield, respectively, indicating that the proposed quadratic model was significant and validated. The statistical analysis of experimental data depicted increasing the temperature, extraction time, and solvent part. The crystal yield increases as a result of the increased δ value of ethyl acetate (**Fig. 1, Supplementary Fig. 1**). To extract AGL crystals from 1 part of crude drug, approximately 8.6 part of the solvent, 124 °C and approximately 1 hr time were required in direct Soxhlet extraction **(Supplementary Table 2)**.

Identification of andrographolide by HPTLC

Fig. 2 shows that AGL was not extracted in nonpolar solvents due to the considerable variation in the polarity index and the δ value. It is extracted in moderately polar (ethyl acetate) and polar solvents (methanol), which gives a clear spot similar to the R_f (0.28) value of standard AGL.

Quantification of AGL by HPTLC

Based on the observed chromatogram, **fig. 3 and 4** show that the rich fragment of AGL present in Soxhlet ethyl acetate crystal (S5) > Direct Cold Maceration Methanol (S1) > Continuous Cold Maceration Methanol (CCM)> Direct Cold Maceration Ethyl acetate (S2) > Continuous Cold Maceration Ethyl acetate (CEA) > Continuous Soxhlet extraction Methanol (SM)> Continuous Soxhlet extraction Ethyl acetate (SEA)> Direct Soxhlet extraction Ethyl acetate (S4) > Direct Soxhlet extraction Methanol (S3)> Continuous Cold Maceration Toluene (CT). The observed result found that in S5, a pure AGL crystal was obtained, and in other techniques, AGL was present in solubilized form with other polar constituents. Polar solvents such as methanol give better AGL yields at ambient temperature in the cold maceration method; however, moderately polar solvents such as ethyl acetate give pure crystals at elevated temperatures in Soxhlet extraction, and nonpolar solvents such as hexane and pet. Ether and toluene were not suitable for AGL extraction. In cold maceration, a highly polar solvent extracts a high amount of AGL due to a similar δ value, but further separation is required to obtain a pure compound. Ethyl acetate extract obtained from Soxhlet and Cold Maceration was examined. AGL crystals only appeared in the Soxhlet ethyl acetate extract; it inferred that at elevated temperatures, the solubility of AGL increased in ethyl acetate, and upon cooling, it precipitated and appeared in the form of crystals.

Determination of % Purity

Fig. 4 shows that the purest AGL crystal obtained from direct Soxhlet extraction in ethyl acetate ascribes that the polarity of ethyl acetate increases at elevated temperatures and reaches a polarity index similar to that of AGL and pure AGL extract in the form of crystals, revealing that extraction efficiency is highly affected by temperature (Chanioti, Tzia, & Technologies, 2018). In another method, the extract consists of numerous compounds along with AGL. The percentage of AGL present in the different extracts is given in **Fig. 4**; it depicts that variation in polarity by the effect of temperature may affect the extraction of AGL. Quantification of the amorphous extract obtained from different solvents showed that the methanol extract has a rich fragment of AGL compared to ethyl acetate and another solvent, but it requires further purification for the isolation of pure AGL.

Identification of AGL by FT-IR

The crystal peak (S5) appears at 3387 cm^{-1} (-OH stretching), 2925 cm^{-1} (sp^3 C-H stretching), 2846 cm^{-1} (C-H stretching), 1717 cm^{-1} (-COOR stretching), and 1669 cm^{-1} (C=C stretching), as shown in **fig. 5**. All the observed peaks of the crystal (S5/AGL-DSEAC) exactly matched the standard AGL compared to other extracts. Similar peaks were reported by Mishra et al.(P. Singh et al., 2006) for the identification of AGL. Solvent polarity may affect the shift of the FT-IR peak of organic compounds due to solvent interactions, called solvent effects (Allerhand & Schleyer,

1963; I. Singh et al., 2019). Apart from AGL-DSEAC, other extracts show a shifting of the signal compared to the standard peak as a result of solvent interaction and the influence of temperature. The formation of the hydrogen bond with solvents shifted in the FT-IR spectra peak. The AGL-DCMM ester group peak appeared at 1650 cm^{-1}; it shifted to a lower frequency, exhibiting a redshift in the spectra. This might occur due to solvent hydrogen bond interactions with the carbonyl group of AGL.

In AGL-DSEA, the -COOR stretching peak appeared at 1736 cm^{-1} and shifted to a higher frequency concerning AGL-STD as a result of the blueshift, whereas in AGL-DCMEA, the same peaks were observed at 1702 cm$^-$ shifted to a lower frequency in concert with the standard peak as a result of the redshift, which might occur due to the solvent interaction with AGL under the influence of temperature. The shifting of frequency is directly associated with the effect of temperature. The stretching frequency increases with increasing temperature(Brockmeier, 1968). **Fig. 5** shows that methanol and ethyl acetate extracts have characteristic peaks of AGL, and the crystal obtained in ethyl acetate precisely matched the AGL-STD peak, which indicated that the crystal was chemically pure AGL, which was further confirmed by other sophisticated analytical techniques.

Structural elucidation of the andrographolide crystal by NMR

Fig. 6A shows that AGL is a bicyclic diterpenoid lactone with three hydroxyl groups at C-3, C-14, and C-19. Proton present at this respective carbon are secondary, allylic, and primary, respectively. ^{1}H NMR spectra **Fig. 6B** NMR spectra exhibited that S5 three proton signals of alcoholic hydrogen did not appear in the ^{1}H-NMR spectrum; it inferred that alcoholic protons interchanged with the deuterium isotopes of deuterated methanol (CD$_3$OD) used as a solvent. The CD$_3$OD of deuterium isotopes is easily interchanged with the active hydrogen of alcohol protons; as a result, protons are diminished in the ^{1}H-NMR spectrum of AGL (Haslauer, Hemmler, Schmitt-Kopplin, & Heinzmann, 2019). The S5 ^{1}H NMR spectrum depicted 27 hydrogens and the presence of methyl groups H-18 at δ 1.27-1.45 (3H) and H-20 at δ 0.77 (3H). **Fig. 6B** shows signals of the methylene group at aliphatic chain H-11 at δ 2.52-2.71 (2H) and in lactone ring H-15 at δ 4.09-4.20 (2H) and in cyclic hexane ring H-1 at δ 1.27-1.84 (2H), H-2 δ 1.84 (2H), H-6 δ 1.45-1.84 (2H) and H-7 δ 2.08-2.45 (2H). Hydrogen at tertiary carbon appeared at H-5 at δ 1.36 (1H) and H-9 at δ 1.93 (1H). Another characteristic signal of AGL can be confined by the appearance of two double bonds, hydrogen signal H-12 at δ 6.85 (1H) and H-17 at δ 4.69 (2H). The signals appeared at H-3 δ 4.48

(1H), H-14 δ 5.03 (1H), and H-19 δ 3.35-3.48 (2H), indicating that protons were present at secondary, allylic, and primary alcoholic carbons, as shown in **Fig. 6B.** A similar investigation was reported by Levita, Jutti, et al (Levita et al., 2011). The triplet at H-12 δ 6.85 confirms the double bond hydrogen. The diastereotopic methylene protons at H-15a and 15b δ 4.09-4.20 (2H) are similar to the ^{1}H-NMR of andrographolide (Nosáľová et al., 2014). The appearance of the signal at the characteristic δ value indicated that the obtained crystal was andrographolide, and ^{13}C and DEPT 90/135 analysis also confirmed their structure.

Fig. 7A and 7B depict that AGL is a bicyclic diterpenoid lactone with 20 carbons. S5 was further characterized by ^{13}C NMR spectroscopy, and CD$_3$OD was used as a solvent; in this study, the chemical shift values of S5 (Table 02) found lactone carbonyl (C-16) and two methyl groups (C-18, 20) at δ 171.24 and δ 21.97, δ 14.13, respectively (Z. G. Chen, R. X. Tan, & L. J. G. C. Cao, 2009) The characteristic Exo double bond (C-17) at δ 107.81, lactone ring-attached double bond (C-12, C-13) at δ 147.39, 128.41, and an endocyclic double bond at (C-8) δ 147.93. The hydroxyl group attached carbon (C-3, C-14, and C-19) signals are observed at δ 79.53, 65.26, and 63.58 secondary, lactone ring and methylene carbons, respectively. Furthermore, the cyclohexane ring of methylene carbons (C-1, C-2, C-6, and C-7) signals at δ 37.58, 27.64, 24.31, and 36.74 appeared in the ^{13}C NMR spectrum. The methylene carbon (C-15) present in the lactone ring signal shows a field value at δ 74.73 due to the deshielding effect of the ring (Patra et al., 1981). The S5 ^{13}C NMR spectroscopy data of tertiary (C-5) at δ 54.94 and quaternary carbons (C-4, C-10) at δ 42.29, 38.57 were confirmed. All the observed values match the value proposed in **Fig. 7B**; the obtained crystal was pure AGL.

DEPT-90/135 NMR: **Fig. 8 and 9** show that the shifting of a peak in the positive or negative phase complies with the reported value for the standard given in **Table 3** and matches the value predicted by Chem Draw exhibited in **Fig. 6A and 7B**, indicating that the obtained crystal was AGL.

CONCLUSION

The solute: solvent ratio, extraction temperature, and time play a significant role in acquiring the optimum δ value of ethyl acetate at which AGL dissolved and crystallized when the solvent reached ambient temperature. The new finding of the proposed work is to optimize the extraction parameters for a mild polar solvent (ethyl acetate). This finding concludes that a high yield of pure AGL was

extracted in a single stage in a moderately polar solvent compared to previously reported polar solvents (methanol, ethanol). This optimized method can extract pure AGL crystals in a moderately polar solvent by minimizing the polarity index and Hildebrand solubility parameter difference of AGL and ethyl acetate. This method is more economical for pure crystal isolation, and in other extraction methods, multiple components were obtained along with AGL. The AGL extraction percentage varies with extraction parameters (polarity of solvents, temperature) and methods. Ethyl acetate is a good choice as the solvent in the Soxhlet method, and methanol is a good choice for the Maceration method to extract AGL.

ABBREVIATIONS

AGL, andrographolide; TLC, Thin Layer Chromatography; HPTLC, High-Performance Thin Layer Chromatography; UV, Ultra Violet; FT-IR, Fourier Transform Infrared; NMR, Nuclear Magnetic Resonance.

Supportive Link

10.6084/m9.figshare.21687314

REFERENCES

Allerhand, A., & Schleyer, P. v. R. J. J. o. t. A. C. S. (1963). Solvent effects in infrared spectroscopic studies of hydrogen bonding. *Journal of the American Chemical Society, 85*(4), 371-380.

Ballesteros-Vivas, D., Álvarez-Rivera, G., Morantes, S. J., del Pilar Sánchez-Camargo, A., Ibáñez, E., Parada-Alfonso, F., & Cifuentes, A. (2019). An integrated approach for the valorization of mango seed kernel: Efficient extraction solvent selection, phytochemical profiling and antiproliferative activity assessment. *Food Research International, 126*, 108616.

Barwick, V. J. (1997). Strategies for solvent selection—a literature review. *TrAC Trends in Analytical Chemistry, 16*(6), 293-309.

Brockmeier, N. F. J. J. o. A. P. S. (1968). The effect of temperature on the infrared absorption frequencies of polyethylene and ethylene–propylene copolymer films. *Journal of Applied Polymer Science, 12*(9), 2129-2140.

Chanioti, S., Tzia, C. J. I. F. S., & Technologies, E. (2018). Extraction of phenolic compounds from olive pomace by using natural deep eutectic solvents and innovative extraction techniques. *Innovative Food Science, 48*, 228-239.

Chen, Z. G., Tan, R. X., & Cao, L. (2009). Efficient and highly regioselective acylation of andrographolide catalyzed by lipase in acetone. *Journal of Green Chemistry, 11*(11), 1743-1745.

Chen, Z. G., Tan, R. X., & Cao, L. J. G. C. (2009). Efficient and highly regioselective acylation of andrographolide catalyzed by lipase in acetone. *Green Chemistry, 11*(11), 1743-1745.

Du Q, J. G., Winterhalter P. . (2003). Separation of andrographolide and neoandrographolide from the leaves of Andrographis paniculata using high-speed counter-current chromatography. *Journal of Chromatography A., 984*(1), 147-151.

Haslauer, K. E., Hemmler, D., Schmitt-Kopplin, P., & Heinzmann, S. S. J. A. C. (2019). Guidelines for the Use of Deuterium Oxide (D2O) in 1H NMR Metabolomics. *Analytical Chemistry, 91*(17), 11063-11069.

Kumoro, A., & Hasan, M. J. C. J. o. C. E. (2007). Supercritical carbon dioxide extraction of andrographolide from Andrographis paniculata: effect of the solvent flow rate, pressure, and temperature. *Chinese Journal of Chemical Engineering, 15*(6), 877-883.

Lapornik, B., Prošek, M., & Wondra, A. G. (2005). Comparison of extracts prepared from plant by-products using different solvents and extraction time. *Journal of food engineering, 71*(2), 214-222.

Levita, J., Widiastuti, N. M., Nugrahani, I., Musadad, A., Mutalib, A., & Ibrahim, S. J. I. J. o. C. (2011). Indirect iodination on the vinyl double bond of andrographolide. *International Journal of Chemistry, 3*(4), 47.

Liu, M., Chen, H., Chen, L., Jiang, H., Liu, R., Pei, Z., . . . Xu, H. (2022). Andrographolide liquisolid using porous-starch as the adsorbent with enhanced oral bioavailability in rats. *Journal of Pharmaceutical Sciences*.

Mahato, S. B., & Kundu, A. P. (1994). 13C NMR spectra of pentacyclic triterpenoids—a compilation and some salient features. *Journal of Phytochemistry, 37*(6), 1517-1575.

Mohan, M., Huang, K., Pidatala, V. R., Simmons, B. A., Singh, S., Sale, K. L., & Gladden, J. M. (2022). Prediction of solubility parameters of lignin and ionic liquids using multi-resolution simulation approaches. *Journal of Green Chemistry, 24*(3), 1165-1176.

Mohan, M., Khanam, S., Shivananda, B. J. J. o. P., & Phytochemistry. (2013). Optimization of

microwave assisted extraction of andrographolide from Andrographis paniculata and its comparison with refluxation extraction method. *Journal of Pharmacognosy Phytochemistry, 2*(1).

Nosáľová, G., Majee, S. K., Ghosh, K., Raja, W., Chatterjee, U. R., Jureček, Ľ., & Ray, B. J. I. j. o. b. m. (2014). Antitussive arabinogalactan of Andrographis paniculata demonstrates synergistic effect with andrographolide. *International journal of biological macromolecules, 69*, 151-157.

Patra, A., Mitra, A. K., Biswas, S., Gupta, C. D., Basak, A., & Barua, A. J. O. M. R. (1981). Carbon-13 NMR spectral studies on some labdane diterpenoids. *Organic Magnetic Resonance, 16*(1), 75-77.

Paul, A., Vibhuti, A., & Raj, V. S. (2021). Evaluation of antiviral activity of Andrographis paniculata and Tinospora cordifolia using in silico and in vitro assay against DENV-2. *Journal of Pharmacognosy Phytochemistry, 10*(2), 486-496.

Rafińska, K., Pomastowski, P., Rudnicka, J., Krakowska, A., Maruśka, A., Narkute, M., & Buszewski, B. J. F. c. (2019). Effect of solvent and extraction technique on composition and biological activity of Lepidium sativum extracts. *Food chemistry, 289*, 16-25.

Rahul, M., Boini, T., Lakshminarayana, M., Radhakrishnan, T., & Sudayadas, R. K. (2022). Approaches to Improve Solubility, Stability and the Clinical Potential of Andrographolide: A Review. *Journal of Young Pharmacists, 14*(1), 15.

Rezaei, H., Rahimpour, E., Zhao, H., Martinez, F., & Jouyban, A. J. J. o. M. L. (2021). Solubility measurement and thermodynamic modeling of caffeine in N-methyl-2-pyrrolidone+ isopropanol mixtures at different temperatures. *Journal of Molecular Liquids, 336*, 116519.

Roth, M. J. M. (2019). Cohesive energy densities versus internal pressures of near and supercritical fluids. *Molecules, 24*(5), 961.

Rubi, R. V. C., Quitain, A. T., Agutaya, J. K. C. N., Doma Jr, B. T., Soriano, A. N., Auresenia, J., & Kida, T. (2019). Synergy of in-situ formation of carbonic acid and supercritical CO2-expanded liquids: Application to extraction of andrographolide from Andrographis paniculata. *The Journal of Supercritical Fluids, 152*, 104546.

Sharma, S., & Sharma, Y. P. J. A. o. P. (2018). Comparison of different extraction methods and HPLC method development for the quantification of andrographolide from Andrographis paniculata (Burm. f.) Wall. ex Nees. *Annals of Phytomedicine, 7*(1), 119-130.

Singh, I., El-Emam, A. A., Pathak, S. K., Srivastava, R., Shukla, V. K., Prasad, O., & Sinha, L. J. M. S. (2019). Experimental and theoretical DFT (B3LYP, X3LYP, CAM-B3LYP and M06-2X) study on electronic structure, spectral features, hydrogen bonding and solvent effects of 4-methylthiadiazole-5-carboxylic acid. *Molecular Simulation, 45*(13), 1029-1043.

Singh, P., Hasan, T., Prasad, O., Sinha, L., Raj, K., & Misra, N. J. S. (2006). FT-IR spectra and vibrational spectroscopy of Andrographolide. *Spectroscopy, 20*(5-6), 275-283.

Sodeifian, G., Alwi, R. S., Razmimanesh, F., & Tamura, K. (2021). Solubility of quetiapine hemifumarate (antipsychotic drug) in supercritical carbon dioxide: Experimental, modeling and hansen solubility parameter application. *Journal Fluid Phase Equilibria, 537*, 113003.

Sohani, A., Pedram, M. Z., Berenjkar, K., Sayyaadi, H., Hoseinzadeh, S., Kariman, H., & Assad, M. E. H. (2021). Techno-energy-enviro-economic multi-objective optimization to determine the best operating conditions for preparing toluene in an industrial setup. *Journal of Cleaner Production, 313*, 127887.